INTERNATIONAL STANDARD

ISO 16063-13

First edition
2001-12-01

Methods for the calibration of vibration and shock transducers —

Part 13:
Primary shock calibration using laser interferometry

Méthodes pour l'étalonnage des transducteurs de vibrations et de chocs —

Partie 13: Étalonnage primaire de chocs par interférométrie laser

Reference number
ISO 16063-13:2001(E)

ISO copyright office
Case postale 56 • CH-1211 Geneva 20
Tel. + 41 22 749 01 11
Fax + 41 22 749 09 47
E-mail copyright@iso.ch
Web www.iso.ch

Printed in Switzerland

Contents

Page

Annexes

Foreword

ISO (the International Organization for Standardization) is a worldwide federation of national standards bodies (ISO member bodies). The work of preparing International Standards is normally carried out through ISO technical committees. Each member body interested in a subject for which a technical committee has been established has the right to be represented on that committee. International organizations, governmental and non-governmental, in liaison with ISO, also take part in the work. ISO collaborates closely with the International Electrotechnical Commission (IEC) on all matters of electrotechnical standardization.

International Standards are drafted in accordance with the rules given in the ISO/IEC Directives, Part 3.

Draft International Standards adopted by the technical committees are circulated to the member bodies for voting. Publication as an International Standard requires approval by at least 75 % of the member bodies casting a vote.

Attention is drawn to the possibility that some of the elements of this part of ISO 16063 may be the subject of patent rights. ISO shall not be held responsible for identifying any or all such patent rights.

International Standard ISO 16063-13 was prepared by Technical Committee ISO/TC 108, *Mechanical vibration and shock*, Subcommittee SC 3, *Use and calibration of vibration and shock measuring instruments*.

ISO 16063 consists of the following parts, under the general title *Methods for the calibration of vibration and shock transducers*:

— *Part 1: Basic concepts*

— *Part 11: Primary vibration calibration by laser interferometry*

— *Part 12: Primary vibration calibration by the reciprocity method*

— *Part 13: Primary shock calibration using laser interferometry*

— *Part 21: Secondary vibration calibration by comparison*

Annex A forms a normative part of this part of ISO 16063. Annexes B and C are for information only.

Introduction

The shock sensitivity S_{sh} is determined, according to definition, as the relationship between the peak values of the accelerometer output quantity and the acceleration. S_{sh} is not a unique quantity but may vary depending on the duration and shape of the shock pulse and the bandwidth over which the sensitivity of the transducer under test and the frequency response of the optional conditioning amplifier are sufficiently uniform.

A unique quantity applicable for linearity tests of accelerometers is the complex sensitivity at a frequency f_n, calculated in the frequency domain. This part of ISO 16063 makes use of data-processing procedures which allow the magnitude S_n and phase shift $\Delta\varphi_n$ of the complex sensitivity to be calculated, in addition or alternatively to the shock sensitivity S_{sh} (cf. informative annex C).

The method specified in this part of ISO 16063 is based on the absolute measurement of the time history of the motion. This method fundamentally deviates from another shock calibration method which is based on the principle of the change in velocity, described in ISO 16063-1. The shock sensitivity therefore differs fundamentally from the shock calibration factor obtained by the latter method, but is in compliance with the calibration factor stated in ISO 5347-4[1].

1) To be revised as ISO 16063-22.

Methods for the calibration of vibration and shock transducers —

Part 13: Primary shock calibration using laser interferometry

1 Scope

This part of ISO 16063 specifies the instrumentation and procedure to be used for primary shock calibration of rectilinear accelerometers, using laser interferometry to sense the time-dependent displacement during the shock. The method is applicable in a shock pulse duration range 0,05 ms to 10 ms and a range of peak values of 10^2 m/s^2 to 10^5 m/s^2 (pulse-duration dependent). The method allows the shock sensitivity to be obtained.

2 Normative references

The following normative documents contain provisions which, through reference in this text, constitute provisions of this part of ISO 16063. For dated references, subsequent amendments to, or revisions of, any of these publications do not apply. However, parties to agreements based on this part of ISO 16063 are encouraged to investigate the possibility of applying the most recent editions of the normative documents indicated below. For undated references, the latest edition of the normative document referred to applies. Members of ISO and IEC maintain registers of currently valid International Standards.

ISO 5347-22, *Methods for the calibration of vibration and shock pick-ups — Part 22: Accelerometer resonance testing — General methods*

ISO 16063-1, *Methods for the calibration of vibration and shock transducers — Part 1: Basic concepts*

ISO 16063-11, *Methods for the calibration of vibration and shock transducers — Part 11: Primary vibration calibration by laser interferometry*

3 Uncertainty of measurement

The limits of the uncertainty of shock sensitivity measurement shall be as follows:

— 1 % of the reading at a reference peak value of 1 000 m/s^2 and reference shock pulse duration of 2 ms and reference amplifier gain settings;

— $\leqslant$ 2 % for all values of peak acceleration and shock pulse duration.

The uncertainty specifications above are valid for the calibration of acceptable precision-grade transducers (e.g. reference standard accelerometers) provided that great care is taken to keep all uncertainty components small enough to comply with the specifications (for uncertainty budgets, see annex A). In particular, the spectral energy produced by the excitation of any mode of resonance inherent in the transducer or shock machine structure during calibration must be small relative to the spectral energy contained in the frequency range of calibration. The transducer resonance testing shall be performed in accordance with ISO 5347-22. In general, this requirement might preclude the use of pulses with relatively short durations that are given in clauses 1 and 6.

All users of this part of ISO 16063 shall make uncertainty budgets according to annex A to document their level of uncertainty.

NOTE The uncertainty of measurement is expressed as the expanded measurement uncertainty in accordance with ISO 16063-1 (briefly referred to as “uncertainty”).

4 Requirements for apparatus

4.1 General

This clause gives specifications for the apparatus necessary to fulfil the scope of clause 1 and to obtain the uncertainties of clause 3.

4.2 Shock machine based on rigid body motion of an anvil

The shock machine shall be operated with a hammer (projectile) which shall be permitted to move and strike an anvil (target) to which the accelerometer is attached. The hammer shall impart a motion to the anvil which shall be permitted to accelerate freely and rectilinearly while the hammer shall be automatically caught. Steel springs or cushioning pads made of rubber, paper or another pulse-forming material shall be placed between the hammer and the anvil to obtain the desired pulse duration and shape. The shock pulses obtained shall have a shape approximating a half-sine, half-sine squared or Gaussian acceleration shape. The resonance frequencies of the hammer and the anvil shall be at least $10/T$, where T is the pulse duration.

In order to avoid influences from resonances in the shock machine structure, the hammer and the anvil shall operate largely isolated from the structure. The hammer and the anvil shall be aligned with a maximum distance of $\pm$ 0,2 mm between the two centrelines. The anvil shall be supported in such a way that no unsymmetric forces cause rotation and deviations from rectilinear motion.

The surface on which the accelerometer is to be mounted shall have a roughness value, expressed as the arithmetical mean deviation, Ra, of $<$ 1 µm.

The flatness shall be such that the surface is contained between two parallel planes at a distance apart of 5 µm, over the area corresponding to the maximum mounting surface of any transducer to be calibrated.

The drilled and tapped hole for connecting the accelerometer shall have a perpendicular tolerance to the surface of $<$ 10 µm; i.e. the centreline of the hole shall be contained in a cylindrical zone of 10 µm diameter and a height equal to the hole depth.

NOTE 1 The above requirements can be fulfilled when the anvil or both the anvil and the hammer is (are) equipped with air bearings (cf. Figure 1 and reference [1]). The shock machine shown in Figure 1 allows impulses of a half-sine squared acceleration shape to be generated [6].

NOTE 2 Some conventional shock machines used in comparison shock calibrations in accordance with ISO 5347-4 (cf. [2] and [3]) may not cause a motion which can be accurately measured by laser interferometry.

4.3 Shock machine based on wave propagation inside a long thin bar

The shock machine shall consist mainly of a movable element [e.g. a steel ball (projectile)] which shall be accelerated to strike a mitigating element (e.g. a steel ball of the same diameter) attached to a bar on which the accelerometer shall be mounted at the opposite end surface. The bar shall be flexibly supported in such a way that influences from resonances in the shock machine structure are avoided. The hammer and the anvil bar shall be aligned sufficiently to meet the uncertainty requirements of clause 3.

Any deviations from the rectilinear motion of the accelerometer's mounting surface shall be so small, at least during the measurement period which is significant for the data acquisition (maximum: 1 ms), that the stated uncertainty in calibration can be achieved. The shock machine shall be provided with a facility for triggering the data acquisition process.

The surface on which the accelerometer is to be mounted shall have a roughness value, expressed as the arithmetical mean deviation, Ra, of $<$ 1 µm.

The flatness shall be such that the surface is contained between two parallel planes at a distance apart of 5 µm, over the area corresponding to the maximum mounting surface of any transducer to be calibrated.

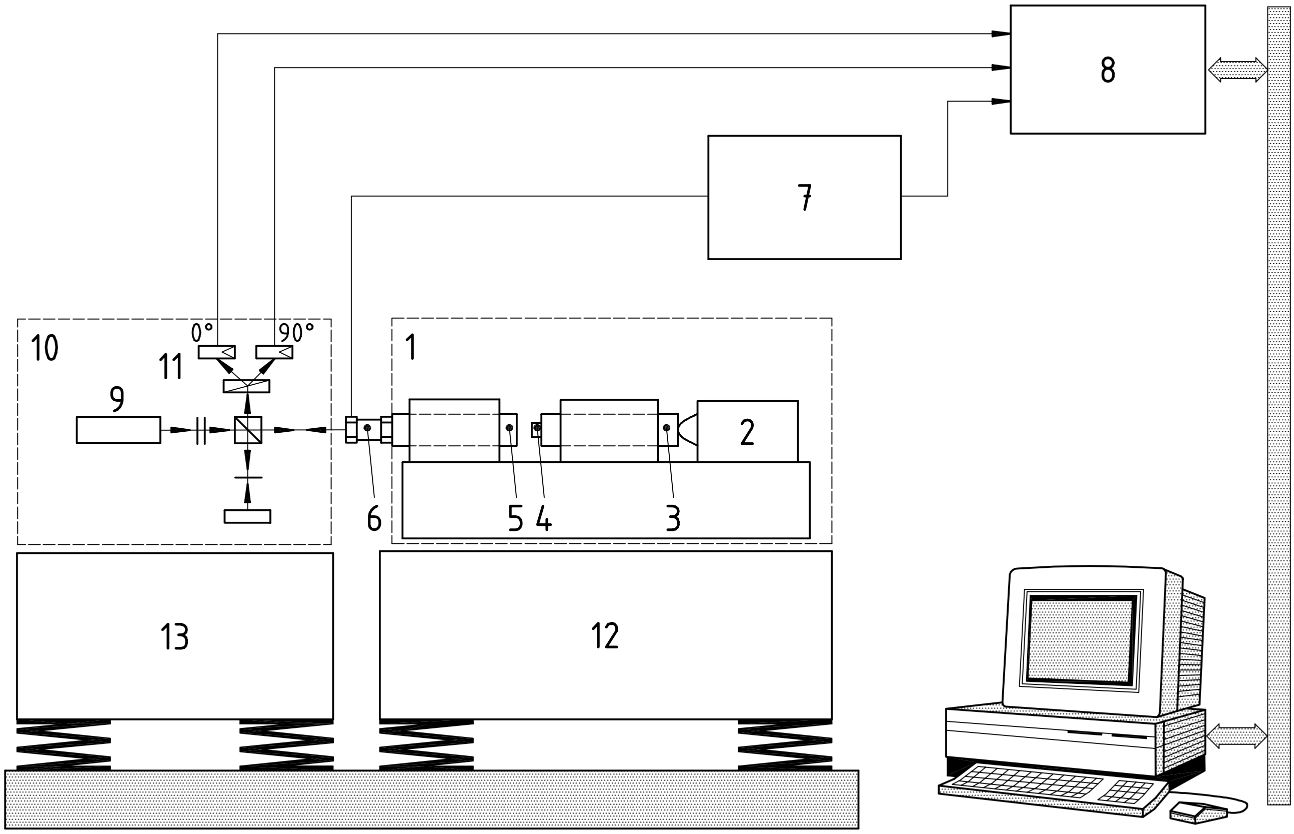

Key

1 Shock machine (4.2)
2 Spring unit
3 Airborne hammer (e.g. steel, diameter 30 mm, length 200 mm)
4 Pad
5 Airborne anvil (e.g. steel, diameter 30 mm, length 200 mm)
6 Accelerometer
7 Amplifier
8 Digital waveform recorder (4.8)
9 Laser (4.5)
10 Interferometer (4.6)
11 Light detectors (4.6)
12 1st seismic block (4.4)
13 2nd seismic block (4.4)

Figure 1 — Example of a measuring system for shock calibration based on rigid body motion of an anvil (acceleration peak value range 100 m/s^2 to 5 000 m/s^2)

The drilled and tapped hole for connecting the accelerometer shall have a perpendicularly tolerance to the surface of $< 10\ \mu m$, i.e. the centreline of the hole shall be contained in a cylindrical zone of 10 µm diameter and a height equal to the hole depth.

The dimension of the bar (see references [4], [5]) shall take into account the fact that the end surface must be accessible to the laser light beam when an accelerometer of single-ended design is mounted for calibration, and that the period available (see below) is sufficient.

The maximum shock duration and measurement period available for data acquisition is the period from the beginning of the significant pulse to the occurrence of the pulse reflected at the mounting surface (e.g. 0,8 ms in a bar 2 m in length as shown in Figure 2).

An example of a shock machine based on elastic wave propagation inside a long thin bar is shown in Figure 2. To derive a trigger signal, two strain gauges are applied to the opposite sides of the bar. The shock excitation arrangement with two steel balls shown in Figure 2 leads to acceleration shapes which can be described by the derivative of a Gaussian function, i.e. Gaussian velocity pulse [6]. This special arrangement gives good repeatability in repeated shock calibrations and relatively small changes of the spectral frequency content of the shock spectrum at different acceleration peak values [13]. Other bar sizes than that shown in Figure 2 may be applied in adaptation to different calibration conditions.

In general, the longitudinal displacement in the bar will vary as a complicated function of radial position and frequency depending on the material properties and diameter of the bar. This can introduce a frequency-dependent base strain to the transducer under test, increase the uncertainty in the calibration, or both.

4.4 Seismic block(s) for shock machine and laser interferometer

The shock exciter and the interferometer shall be mounted on the same heavy block or on two different heavy blocks so as to prevent relative motion due to ground motion, or to prevent the reaction of the exciter support structure from having excessive effects on the calibration results.

4.5 Laser

A laser of the red helium-neon type shall be used. Under laboratory conditions, i.e. an air pressure of 100 kPa, a temperature of 23 °C and a relative humidity of 50 %, the wavelength is 0,632 81 µm.

If the laser has manual or automatic atmospheric compensation, this shall be set to zero or switched off.

Alternatively, a single-frequency laser may be used, with another stable wavelength whose value is accurately known.

4.6 Interferometer

The interferometer shall be of a modified Michelson type, providing quadrature signal outputs, with two light detectors to sense the interferometer signal bands, and having a frequency response covering the necessary bandwidth. The required bandwidth can be calculated from the maximum velocity v_{max}, which shall be measured using the following equation:

$$f_{\text{max}} = v_{\text{max}} \times 3{,}16 \times 10^{-6}\ \text{m}^{-1}$$

The modified Michelson interferometer may be constructed according to Figure 3. A quarter-wavelength retarder converts the linearly polarized incident light into two measuring beams with perpendicular polarization states and a phase angle difference of 90°. After interfering with the linearly polarized reference beam, the two components with perpendicular polarization are separated in space by appropriate means (e.g. a Wollaston prism or a polarizing beam splitter) and detected by two photodiodes.

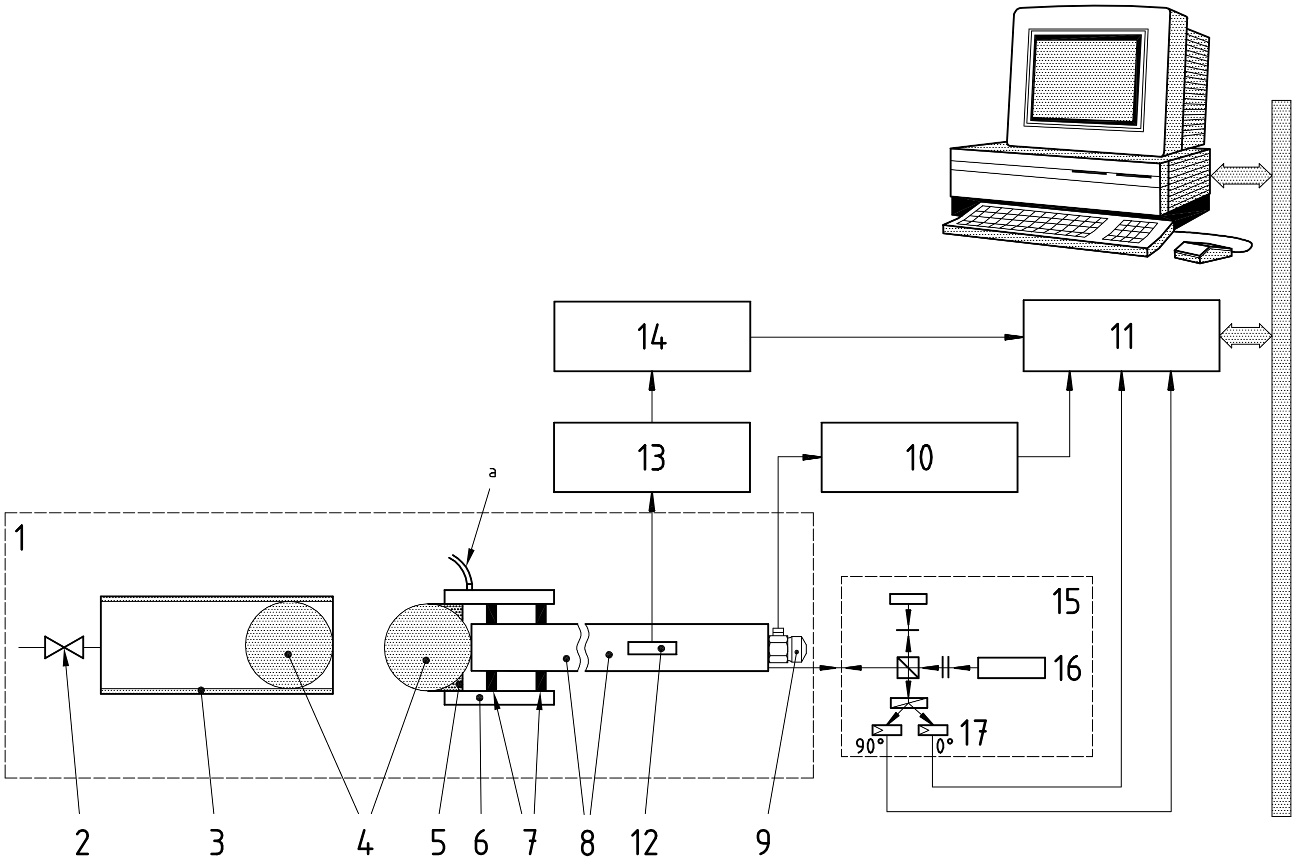

Key

1 Shock machine (4.3)
2 Valve (compressed air supply)
3 Air barrel
4 Pair of balls, of 50 mm diameter
5 Silicon rubber
6 Aluminium tube
7 O-rings
8 Bar (titanium, diameter 25 mm, length 2 000 mm)
9 Accelerometer
10 Amplifier
11 Digital waveform recorder (4.8)
12 Strain gauges
13 Bridge amplifier
14 Trigger unit
15 Interferometer (4.6)
16 Laser (4.5)
17 Light detectors (4.6)

[a] To vacuum

Figure 2 — Example of a measuring system for shock calibration based on shock propagation inside a long thin bar (acceleration peak value range 1 000 m/s^2 to 100 000 m/s^2)

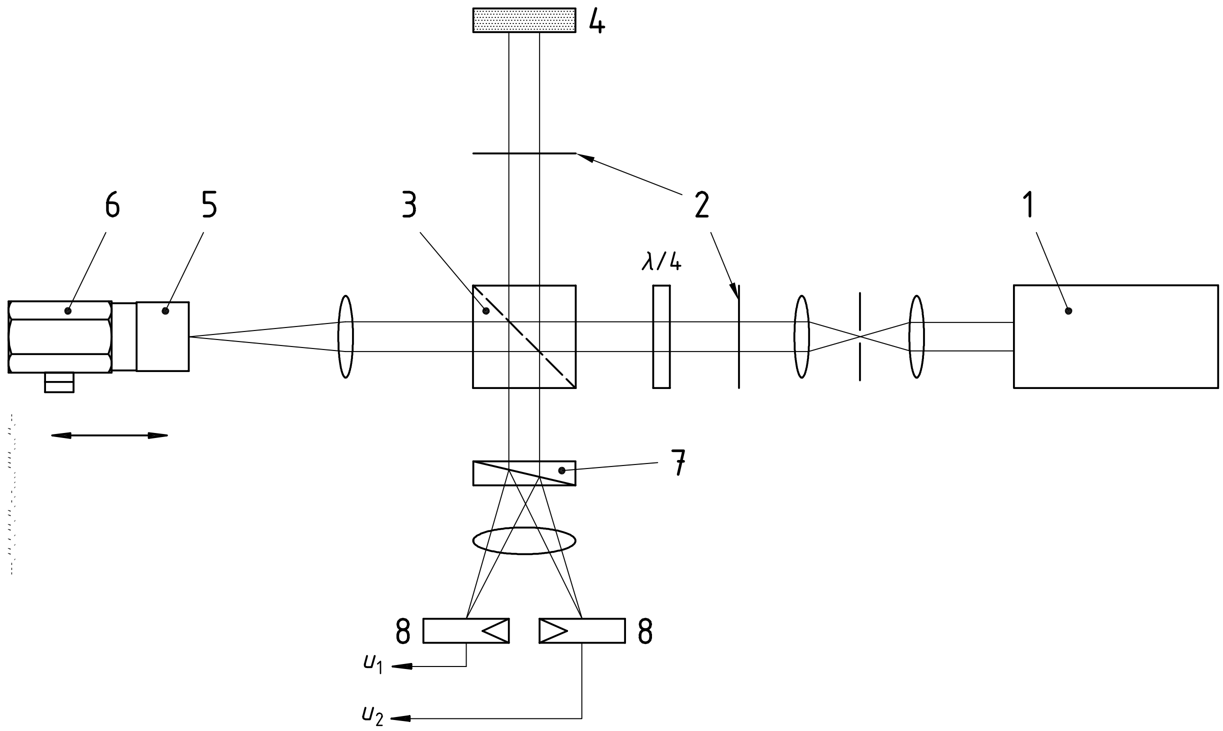

Key

1 Laser
2 Polarizors
3 Beamsplitter
4 Reference mirror
5 Dummy mass (measuring reflector)
6 Accelerometer
7 Wollaston prism
8 Photodetectors

Figure 3 — Laser interferometer with quadrature output

The two outputs of the modified Michelson interferometer shall have offsets of less than $\pm$ 5 % in relation to the amplitude, relative amplitude deviations of less than $\pm$ 5 %, and deviations of less than $\pm$ 5° from the nominal phase angle difference of 90°. To maintain these tolerances, appropriate means shall be provided to adjust the offset, the signal level and the angle between the two interferometer signals.

The measuring light beam from the interferometer and the anvil bar axis shall be aligned to meet the uncertainty requirements of clause 3.

For reflection of the measuring light beam, the polished end surface of the anvil bar shall be used if the accelerometer is of single-ended design, or a polished top surface shall be used in the case of back-to-back accelerometer design. The use of a mirror shall be avoided.

At high acceleration peak values, a large bandwidth may be needed. To measure, for example, a shock of 100 000 m/s^2 peak value and 200 µs duration (for acceleration shape see 4.3), an interferometer signal frequency spectrum up to 32 MHz should be transmitted. For details, see reference [6].

The (modified) Michelson interferometer may be replaced by another suitable two-beam interferometer, e.g. a (modified) Mach-Zehnder interferometer.

4.7 Oscilloscope

Unless included in 4.8, an oscilloscope shall be provided for checking the waveforms of the interferometer and accelerometer signals, with a frequency range from d.c. to 50 MHz or higher.

4.8 Waveform recorder with computer interface

A waveform recorder with computer interface capable of analog-to-digital conversion and storage of the two interferometer quadrature outputs together with the accelerometer output shall be provided. The amplitude resolution, the sampling rate and the memory shall be sufficient for calibration in the intended dynamic range with the uncertainty specified in clause 3. For the interferometer quadrature signal outputs, a resolution of $\geqslant$ 8 bits is sufficient. Typically, an amplitude resolution of $\geqslant$ 10 bits is used for the accelerometer output. A two-channel waveform recorder may be used for the interferometer output signals, together with another waveform recorder (with higher resolution and lower sampling rate) for the accelerometer output signal.

EXAMPLE To calibrate an accelerometer at an acceleration peak value of 2 500 m/s^2 and a pulse duration of 2 ms, a sampling frequency of 50 MHz or higher should be used (a memory of 1 Mbyte being sufficient to cover the three signal channels).

4.9 Computer with data-processing program

A computer with data-processing program according to the procedure for the calculations stated in 7.3 shall be provided.

4.10 Filters

Analog filters applied to the accelerometer output signal and the interferometer signals to avoid aliasing and/or to suppress noise, shall have an appropriate amplitude- and phase-frequency response to comply with the tolerable uncertainty of measurement (cf. clause 3). This requirement shall also be fulfilled for the digital filtering in accordance with the procedures for data processing (cf. 7.3).

For the filtering of the interferometer signals, the error description reported in reference [6] should be taken into account.

4.11 Other requirements

In order to achieve a small measurement uncertainty in calibration (e.g. 1 %), the accelerometer and the accelerometer amplifier should preferably be considered as a single unit and calibrated together.

The accelerometer shall be structurally rigid. The base strain sensitivity, the transverse sensitivity and the stability of the accelerometer/amplifier combination shall be taken into account when calculating the uncertainty of measurement (cf. annex A).

If a back-to-back reference standard accelerometer is calibrated, its sensitivity (magnitude and/or phase shift) shall be measured with a dummy mass that is the equivalent of the mass of the transducer to be calibrated by the comparison method (cf. ISO 5347-4) using the back-to-back reference accelerometer. The laser light spot may be at either the top (outer surface) of the dummy mass or the top surface of the reference standard accelerometer.

If the motion is sensed at the top of the dummy mass, then the dummy mass should have an optically polished top surface and the position of the laser-light spot should be close to the geometrical centre of this surface. In cases where the motion of the mass departs from that of a rigid body, the relative motion between the top (sensed) and bottom surfaces shall be taken into consideration.

Alternatively, the motion may be sensed at the top surface of the reference accelerometer via longitudinal holes in the dummy mass.

In some conventional shock machines used in comparison shock calibrations, the motion of the accelerometer to be calibrated is sensed with the base surface of a back-to-back reference accelerometer, both accelerometers being mounted on a rigid structure. In this case, the back-to-back reference accelerometer shall be calibrated with the shock motion being sensed at the moving part (e.g. the end surface of the bar) close to the accelerometer.

5 Ambient conditions

Calibration shall be carried out under the following ambient conditions:

a) room temperature: (23 ± 3) °C;

b) relative humidity: max. 75 %.

6 Preferred accelerations and pulse durations

The nominal values of acceleration (peak values) and shock pulse duration should preferably be chosen from the following series.

a) **Acceleration**, in metres per second squared:

100; 200; 500; 1 000; 2 000; 5000; 10 000; 20 000; 50 000; 100 000.

b) **Shock pulse duration**, in milliseconds:

0,05; 0,1; 0,2; 0,5; 1; 2; 5; 10.

CAUTION — To avoid damage to the accelerometer, the duration of the calibration shock pulse should be greater than the shortest shock pulse duration specified by the manufacturer.

7 Method

7.1 Test procedure

The equipment should be installed according to Figures 1 or 2, and Figure 3.

The laser interferometer (for an example, see Figure 3) shall be adjusted to give output signals u_1 and u_2 in phase quadrature within the tolerances stated in 4.6.

Before applying a shock, disturbing quantities such as hum and noise shall be measured, and the values shall be sufficiently small to achieve the required uncertainty of calibration.

After the interferometer settings (4.6) have been optimized and the required standard position of the amplifier range switch selected, the shock calibration of the accelerometer shall be carried out at the specified accelerations and pulse durations (see clause 6) as described in 7.2 and 7.3.

NOTE 1 Quadrature signals free from the disturbing parameters tolerated in 4.6 can be generated by digital signal processing in conjunction with special heterodyne interferometer technique as reported in references [7] and [8]. In this way, an uncertainty smaller than that obtained by homodyne technique can be achieved. A suitable heterodyne technique has also special advantages in the photoelectric transmission of interferometer signals of large bandwidth (cf. 4.6), but is considerably more expensive than the homodyne technique.

NOTE 2 To measure the time-varying acceleration, the generation of quadrature signals may be dispensed with when the following means are used: a one-channel Michelson interferometer, a time interval analyser and special algorithms for determining the acceleration values from the measured displacement values and conjugate times (cf. ISO 16063-1; for details see reference [9]).

7.2 Data acquisition

The cut-off frequencies of low-pass filters and, if any, high-pass filters shall be chosen so that disturbing influences from low- and high-pass filtering on the calibration results are tolerable (cf. reference [6]). To fulfil Nyquist's theorem, the sampling rate shall be set so that the highest frequency content is lower than half the sampling rate.

The quadrature signals shall be equidistantly sampled during a measurement period $t_0 < t < t_0 + T_{\text{Meas}}$ with t_0 the start point and $t_0 + T_{\text{Meas}}$ the end point of the data acquisition. The measurement period shall start before the shock pulse occurs at the mounting surface of the accelerometer (recommended time shift: 0,1T, where T is the pulse duration) and shall end before the reflected pulse arrives (recommended time shift: 0,05T).

The series of measurement values $\{u_1(t_i)\}$ and $\{u_2(t_i\}$ sampled within $t_0 < t < t_0 + T_{\text{Meas}}$ shall have a sampling interval $\Delta t = t_i - t_{i-1} =$ const.

The sampled series of accelerometer output values is $\{u(t_i)\}$.

The data shall be transferred to the computer memory.

7.3 Data processing

7.3.1 General

Examples of methods for data processing to calculate the shock sensitivity (peak value of accelerometer output to peak value of acceleration, cf. Introduction) are given in Figure 4 in three possible versions either with or without the use of a discrete Fourier transform (DFT):

a) version without DFT;

b) version with DFT of the velocity values;

c) version with DFT of the displacement values.

For both versions a) and b), most of the calculation steps are common differing only in that the series of acceleration values $a(t_i)$ are calculated from the series of velocity values $v(t_i)$ by differentiation in the time domain or in the frequency domain. In the latter case, discrete Fourier transform (DFT) and inverse discrete Fourier transform (IDFT) are used, and intermediate data are available which may be used for the magnitude of sensitivity and the phase calibration of accelerometers (cf. informative annex C). Version c) uses the frequency domain, exclusively, for the double differentiation leading from the series of displacement values $s(t_i)$ to the series of acceleration values $a(t_i)$.

The version without DFT is applicable to “longer” shocks with $Ta_{\text{peak}} \geqslant 0{,}5$ m/s in the case of sine-squared acceleration shapes (cf. shock machine after 4.2) and $Ta_{\text{peak}} \geqslant 1{,}5$ m/s in the case of Gaussian velocity shapes (cf. shock machine after 4.3), where T is the pulse duration in seconds and a_{peak} is the acceleration peak value in metres per second squared. For shorter shocks, the version with DFT of the velocity values or the version with DFT of the displacement values should be used. These versions are also applicable to shocks of longer pulse duration and may be preferred to suppress efficiently the influence of high-frequency disturbing vibrations, if any. If the velocity of the accelerometer before and after the shock pulse is not zero, a special data-processing procedure (shearing operation) allows the Fourier transform to be correctly applied.

NOTE 1 The relationships and definitions of the shock pulse duration are explained in reference [6]. For the Gaussian velocity shock, the shock pulse duration is the time period within which the velocity is above 0,606 v_{peak}.

NOTE 2 The relationships given above for the shock pulse duration T include the influences of the quadrature signal distortions within the tolerances specified in 4.6 (see reference [6]).

NOTE 3 The product Ta_{peak} approximates the value of the peak velocity. The instantaneous frequency of the interferometer output signal is proportional to the velocity. If the above inequalities are fulfilled, then by the low-pass filtering of the interferometer output signal a sufficient signal-to-noise ratio can be achieved in order to comply with the uncertainty requirements of clause 3.

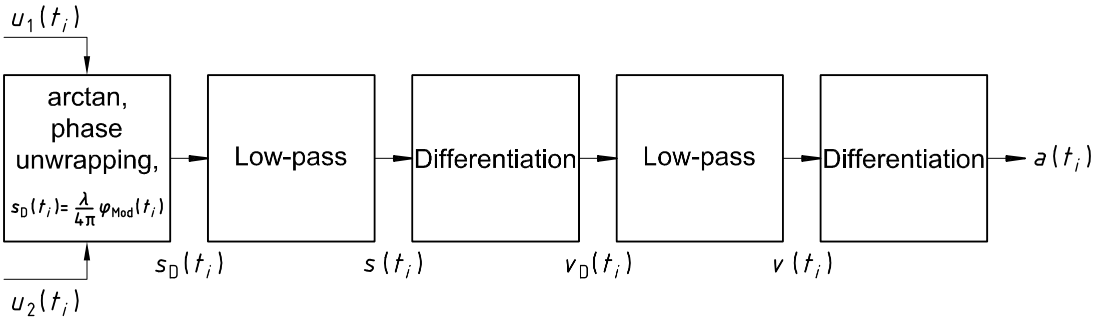

a) Version without DFT

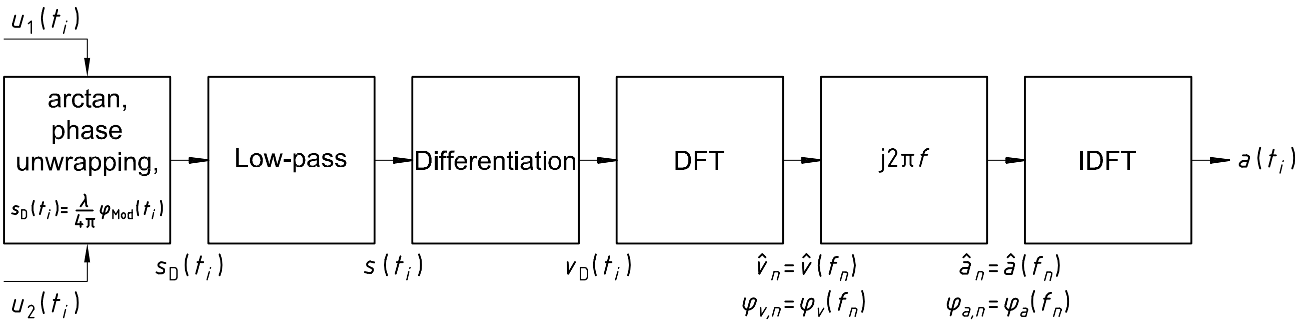

b) Version with DFT of the velocity values

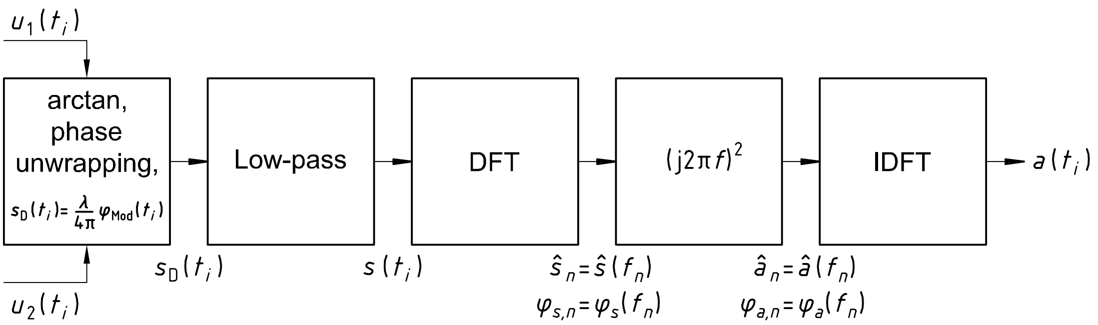

c) Version with DFT of the displacement values

Figure 4 — Signal processing block diagram to obtain shock sensitivity

7.3.2 Calculation of shock sensitivity, version without DFT

The shock sensitivity of the accelerometer shall be calculated by data processing in the following steps a) to i); cf. Figure 4 a).

a) Calculate a series of modulation phase values, $\{\varphi_{\text{Mod}}(t_i)\}$, from the sampled interferometer output values $\{u_1(t_i)\}$ and $\{u_2\,(t_i)\}$ using the formula

$$\varphi_{\text{Mod}}(t_i) = \arctan\frac{u_2(t_i)}{u_1(t_i)} + n\pi \tag{1}$$

where $n = 0,\ 1,\ 2,\ \ldots$.

Choose an integer number n so that discontinuities of $\{\varphi_{\text{Mod}}(t_i)\}$ are avoided for the values $n\pi$.

NOTE A procedure for calculating the number n is described in reference [10].

Calculate a series of displacement values $\{s_{\text{D}}(t_i)\}$ using the formula

$$s_{\text{D}}(t_i) = \frac{\lambda}{4\pi}\,\varphi_{\text{Mod}}(t_i) \tag{2}$$

where the subscript D indicates that the values are distorted by high-frequency noise.

b) Filter the series of displacement values $\{s_{\text{D}}(t_i)\}$ using a digital low-pass filter algorithm and parameters suitable for suppressing high-frequency noise without distorting the signal. The result of filtering is a series of “smooth” displacement values denoted by $\{s(t_i)\}$.

NOTE A filter having monotonous amplitude response (e.g. a recursive Butterworth low-pass of 4th order) is suitable for this purpose. In order to suppress typical noise, the cut-off frequency should be not greater than $16/T$ for sine-squared acceleration shape (cf. 4.2) nor greater than $5/T$ for Gaussian velocity shape (cf. 4.3). The cut-off frequency should not, however, be essentially smaller to keep signal distortion negligible.

c) Calculate the first derivative of the displacement-time function to obtain the velocity-time function as a series of velocity values $\{v_{\text{D}}(t_i)\}$.

NOTE The first derivative at a time t_i can be obtained by the formula

$$v_{\text{D}}(t_i) = \frac{1}{2\Delta t}\,[s(t_i) - s(t_{i-1})] \tag{3}$$

d) Filter the series of velocity values $\{v_{\text{D}}(t_i)\}$ using a digital low-pass filter algorithm and parameters suitable for suppressing high-frequency noise without distorting the signal. The result is a series of “smooth” velocity values denoted by $\{v(t_i)\}$.

The Note given in step b) applies.

e) Calculate the first derivative of the velocity-time function to obtain the acceleration-time function as a series of acceleration values $\{a(t_i)\}$.

NOTE The first derivative at a time t_i can be obtained by the formula

$$a(t_i) = \frac{1}{2\Delta t}\,[v(t_{i+1}) - v(t_{i-1})] \tag{4}$$

f) From the series $\{a(t_i)\}$ of calculated accelerometer input values, select the maximum value, max. $\{a(t_i)\}$, as the peak value a_{peak} of the acceleration.

g) Filter the series of sampled accelerometer output values $\{u_{\text{D}}(t_i)\}$ using a digital low-pass filter algorithm and parameters suitable for suppressing high-frequency noise without distorting the signal. The result of filtering is a series of “smooth” values denoted by $\{u(t_i)\}$.

NOTE A filter having monotonous amplitude response (e.g. a recursive Butterworth low-pass of 4^{th} order) is suitable for this purpose.

h) From the series $\{u(t_i)\}$ of filtered accelerometer output values, select the maximum value, max. $\{u(t_i)\}$, as the peak value u_{peak} of the accelerometer output.

If there is a zero shift in the signal, the zero point immediately before the shock and the shifted zero point immediately after the shock shall be connected by a straight line, this line being the basis for the determination of the output. A maximum zero shift of 1 % relative to the peak value of the output is acceptable. If the zero shift is greater, then its effect on the uncertainty of measurement shall be taken into account and the amount of the zero shift shall be reported.

i) Calculate the shock sensitivity S_{sh} from the values u_{peak}, a_{peak} obtained in h) and f) using the formula

$$S_{\text{sh}} = \frac{u_{\text{peak}}}{a_{\text{peak}}} \tag{5}$$

When the calibration results are reported, the expanded uncertainty of measurement in the calibration shall be calculated and reported in accordance with annex A.

7.3.3 Calculation of shock sensitivity, version with DFT of the velocity values

The shock sensitivity of the accelerometer shall be calculated by data processing in the following steps a) to j); cf. Figure 4 b):

a) as step a) in 7.3.2;

b) as step b) in 7.3.2;

c) as step c) in 7.3.2;

d) calculate the complex frequency spectrum of the velocity by DFT applied to the series of velocity values $\{v(t_i)\}$ obtained in c);

e) multiply the complex velocity spectrum obtained in d) by the complex radian frequency $\text{j}2\pi f$ to obtain the complex frequency spectrum of the acceleration;

f) calculate the series $\{a(t_i)\}$ of acceleration values by IDFT;

g) as step f) in 7.3.2;

h) as step g) in 7.3.2;

i) as step h) in 7.3.2;

j) as step i) in 7.3.2.

7.3.4 Calculation of shock sensitivity, version with DFT of the displacement values

The shock sensitivity of the accelerometer shall be calculated by data processing in the following steps a) to i); cf. Figure 4 c):

a) as step a) in 7.3.2;

b) as step b) in 7.3.2;

c) calculate the complex frequency spectrum of the displacement by DFT applied to the series of displacement values $\{s(t_i)\}$ obtained in b);

d) multiply the complex displacement spectrum obtained in c) by the complex radian frequency squared, $(\text{j}2\pi f)^2$, to obtain the complex frequency spectrum of the acceleration;

e) as step f) in 7.3.3;

f) as step f) in 7.3.2;

g) as step g) in 7.3.2;

h) as step h) in 7.3.2;

i) as step i) in 7.3.2.

8 Reporting the calibration results

When the calibration results are reported, in addition to the calibration method at least the following conditions and characteristics shall be stated.

a) Ambient conditions:

- — temperature of the accelerometer;
- — ambient air temperature.

b) Mounting technique:

- — material of mounting surface;
- — mounting torque (if the accelerometer is stud-mounted);
- — oil or grease (if used);
- — cable fixing;
- — orientation (vertical or horizontal).

c) Dummy mass (if used):

- — material (e.g. steel), dimensions (length, diameter), mass;
- — mounting torque;
- — values of any correction factors for the sensitivity to compensate the effects of relative motion between top and bottom surfaces (whenever used).

d) Laser light reflection:

- — reflector (e.g. polished end surface of bar);
- — position of laser light spot on reflecting surface.

e) All amplifier settings (if adjustable), for example:

- — gain;
- — cut-off frequencies of filters.

f) Calibration result:

- — peak value and shock pulse duration;
- — values of shock sensitivity;
- — expanded uncertainty of measurement, k factor if different from $k = 2$.

Annex A
(normative)

Expression of uncertainty of measurement in calibration

A.1 Calculation of the expanded uncertainty, $U_{\text{rel}}(S_{\text{sh}})$, for the shock sensitivity S_{sh} for given acceleration peak value, shock pulse duration, and settings of amplifier gain and filter cut-off frequencies

The relative expanded uncertainty of measurement of the shock sensitivity, $U_{\text{rel}}(S_{\text{sh}})$, for the acceleration peak value, shock pulse duration, and settings of amplifier gain and filter cut-off frequencies shall be calculated in accordance with ISO 16063-1 from the following formulae:

$$U_{\text{rel}}(S_{\text{sh}}) = k u_{\text{c,rel}}(S_{\text{sh}})$$

$$u_{\text{c,rel}}(S_{\text{sh}}) = \frac{u_{\text{c}}(S_{\text{sh}})}{S_{\text{sh}}} = \frac{1}{S_{\text{sh}}}\sqrt{\sum_{i=1}^{11} u_i^2(S_{\text{sh}})}$$

with the coverage factor $k = 2$.

Table A.1

i	Standard uncertainty component $u(x_i)$	Source of uncertainty	Uncertainty contribution $u_i(y)$
1	$u(u_{\text{peak,V}})$	accelerometer output voltage peak value measurement (waveform recorder; e.g. ADC-resolution)	$u_1(S_{\text{sh}})$
2	$u(u_{\text{peak,F}})$	voltage filtering effect on accelerometer output voltage peak value (frequency band limitation)	$u_2(S_{\text{sh}})$
3	$u(u_{\text{peak,D}})$	effect of voltage disturbance on accelerometer output voltage peak value (e.g. hum and noise)	$u_3(S_{\text{sh}})$
4	$u(u_{\text{peak,T}})$	effect of transverse, rocking and bending acceleration on accelerometer output voltage peak value (transverse sensitivity)	$u_4(S_{\text{sh}})$
5	$u(a_{\text{peak,Q}})$	effect of interferometer quadrature output signal disturbance on acceleration peak value (e.g. offsets, voltage amplitude deviation, deviation from 90° nominal angle difference)	$u_5(S_{\text{sh}})$
6	$u(a_{\text{peak,F}})$	interferometer signal filtering effect on acceleration peak value (frequency band limitation)	$u_6(S_{\text{sh}})$
7	$u(a_{\text{peak,VD}})$	effect of voltage disturbance on acceleration peak value (e.g. random noise in the photoelectric measuring chain)	$u_7(S_{\text{sh}})$
8	$u(a_{\text{peak,MD}})$	effect of motion disturbance on acceleration peak value (e.g. drift; relative motion between the accelerometer reference surface and the spot sensed by the interferometer)	$u_8(S_{\text{sh}})$
9	$u(a_{\text{peak,PD}})$	effect of phase disturbance on acceleration peak value (e.g. phase noise of the interferometer signal)	$u_9(S_{\text{sh}})$
10	$u(a_{\text{peak,RE}})$	residual interferometric effects on acceleration peak value (interferometer function)	$u_{10}(S_{\text{sh}})$
11	$u(S_{\text{sh,RE}})$	residual effects on shock sensitivity measurement (e.g. effect of resonance excitation in the transducer or shock machine, random effect in repeat measurements; experimental standard deviation of arithmetic mean)	$u_{11}(S_{\text{sh}})$

A.2 Calculation of the expanded uncertainty, $U_{\text{rel}}(S_{\text{sh,t}})$, for the shock sensitivity $S_{\text{sh,t}}$ over the complete range of acceleration peak values and shock pulse durations

The expanded uncertainty of measurement of the shock sensitivity, $U_{\text{rel}}(S_{\text{sh}})$, calculated in accordance with A.1, is valid only for the calibration peak value, shock pulse duration, and settings of amplifier gain and filter cut-off frequencies. The relative expanded uncertainty of measurement of the sensitivity $U_{\text{rel}}(S_{\text{sh,t}})$ for the complete range of acceleration peak value and shock pulse duration, at any time during the interval between successive calibrations, shall be calculated in accordance with ISO 16063-1 from the following formulae:

$$U_{\text{rel}}(S_{\text{sh,t}}) = k u_{\text{c,rel}}(S_{\text{sh,t}})$$

$$u_{\text{c,rel}}(S_{\text{sh,t}}) = \frac{u_{\text{c}}(S_{\text{sh,t}})}{S_{\text{sh}}} = \frac{1}{S_{\text{sh}}}\sqrt{\sum_{i=1}^{10} u_i^2(S_{\text{sh,t}})}$$

with the coverage factor $k = 2$.

Table A.2

i	Standard uncertainty component $u(x_i)$	Source of uncertainty	Uncertainty contribution $u_i(y)$
1	$u(S_{\text{sh}})$	uncertainty of shock sensitivity calculated at reference peak value, shock pulse duration and amplifier gain settings in accordance with A.1	$u_1(S_{\text{sh,t}})$
2	$u(e_{\text{T,A}})$	reference amplifier tracking (deviations in gain and phase shift for different amplification settings)	$u_2(S_{\text{sh,t}})$
3	$u(e_{\text{L},f,\text{A}})$	deviation from constant amplitude-frequency characteristic and linear phase-frequency characteristic of reference amplifier	$u_3(S_{\text{sh,t}})$
4	$u(e_{\text{L},f,\text{P}})$	deviation from constant amplitude-frequency characteristic and linear phase-frequency characteristic of reference accelerometer	$u_4(S_{\text{sh,t}})$
5	$u(e_{\text{L},a,\text{A}})$	amplitude linearity deviation of reference amplifier	$u_5(S_{\text{sh,t}})$
6	$u(e_{\text{L},a,\text{P}})$	amplitude linearity deviation of reference accelerometer	$u_6(S_{\text{sh,t}})$
7	$u(e_{\text{I,A}})$	instability of reference amplifier gain, and effect of source impedance on gain and phase shift	$u_7(S_{\text{sh,t}})$
8	$u(e_{\text{I,P}})$	instability of accelerometer sensitivity (magnitude and phase shift)	$u_8(S_{\text{sh,t}})$
9	$u(e_{\text{E,A}})$	environmental effects on gain and phase shift of reference amplifier	$u_9(S_{\text{sh,t}})$
10	$u(e_{\text{E,P}})$	environmental effects on sensitivity (magnitude and phase shift) of reference accelerometer	$u_{10}(S_{\text{sh,t}})$

Annex B
(informative)

Explanation of the procedures

B.1 General

According to ISO 16063-1, the complex acceleration sensitivity $\underline{S_a}$ of an accelerometer is defined for sinusoidal excitation parallel to a specified axis:

$$\underline{S_a} = \widehat{S}_a \mathrm{e}^{\mathrm{j}(\varphi_u - \varphi_a)} \tag{B.1}$$

where

$$\widehat{S}_a = \frac{\widehat{u}}{\widehat{a}} \tag{B.2}$$

$\widehat{S}_a$ is the magnitude of the acceleration sensitivity;

$\widehat{u}$ is the amplitude of the accelerometer sinusoidal output u (preferably output voltage of the accelerometer/amplifier combination);

$\widehat{a}$ is the amplitude of the sinusoidal acceleration a;

φ_u is the zero phase angle of the output;

φ_a is the zero phase angle of the acceleration;

$(\varphi_u - \varphi_a)$ is the phase shift $\Delta\varphi$ of the complex sensitivity,

$$\Delta\varphi = (\varphi_u - \varphi_a) \tag{B.3}$$

Since the magnitude and phase shift of the complex sensitivity are frequency-dependent, they must be determined at any frequency of interest.

Methods for the absolute calibration of accelerometers by sinusoidal excitation are described in ISO 16063-11. The definition and calibration of the (complex) sensitivity is based on the linear systems theory. As long as this theory applies, absolute calibration using shock excitation may be used as an alternative way to determine the magnitude and phase shift of the complex sensitivity. If the accelerometer deviates from ideal amplitude linearity, the shock calibration results may deviate from those of the vibration calibration. The Fourier spectra of the accelerometer input and output may be calculated in accordance with the informative annex C to determine for any frequency component the magnitude of the complex sensitivity according to equation (B.2) and the phase shift according to equation (B.3). By observation of the influence of the acceleration peak value on the magnitude S_n and phase shift $\Delta\varphi_n$ of the complex sensitivity at certain spectral frequencies f_n, deviations from the ideal amplitude linearity of the accelerometer (with or without charge amplifier), if any, can be identified.

According to the scope (cf. clause 1), the shock excitation is used in this part of ISO 16063 to determine the shock sensitivity of an accelerometer (with or without charge amplifier), as the ratio of the peak value of the output to the peak value of the input, for an acceleration of certain parameters (peak value, shock pulse duration and shock pulse shape). In this case, equation (B.2) applies where $\widehat{u}$ and $\widehat{a}$ are replaced by the peak values u_{peak} and a_{peak}, and where the sensitivity is denoted by S_{sh}:

$$S_{\text{sh}} = \frac{u_{\text{peak}}}{a_{\text{peak}}} \tag{B.4}$$

In this case, the sensitivity depends on the shock pulse duration and, if the accelerometer deviates from ideal amplitude linearity, on the peak value.

When the shock machine generates an acceleration $a(t)$, the accelerometer output signal follows the relationship $u\,(t)$.

The output of the first photodetector can be written as follows:

$$u_1(t) = \widehat{u}_1 \cos \varphi_{\mathrm{Mod}}(t) = \widehat{u}_1 \cos\left[\varphi_0 + \varphi_{\mathrm{M}}(t)\right] \tag{B.5}$$

where the modulation phase

$$\varphi_{\mathrm{Mod}} = \varphi_0 + \varphi_{\mathrm{M}}(t) \tag{B.6}$$

is composed of the zero phase angle of the photodetector signal, φ_0, and a modulation term, $\varphi_{\mathrm{M}}(t)$, which is proportional to the displacement $s(t)$:

$$\varphi_{\mathrm{M}} = \frac{4\pi s(t)}{\lambda} \tag{B.7}$$

It is presupposed that there is no time delay between the displacement $s(t)$ and the sinusoidal phase term $\varphi_{\mathrm{M}}(t)$. The following shows how the displacement can be calculated so that the velocity v and the acceleration a can be derived from the displacement s on the basis of the definition:

$$a(t) = \frac{\mathrm{d}v(t)}{\mathrm{d}t} = \frac{\mathrm{d}^2 s(t)}{\mathrm{d}t^2} \tag{B.8}$$

A second photodetector output that is in quadrature is expressed by:

$$u_2(t) = \widehat{u}_2 \sin \varphi_{\mathrm{Mod}}(t) = \widehat{u}_2 \sin\left[\varphi_0 + \varphi_{\mathrm{M}}(t)\right] \tag{B.9}$$

where $\widehat{u}_2 = \widehat{u}_1$.

The quadrature signals are sampled at a constant sampling rate during a measurement period $t_0 < t < t_0 + T_{\mathrm{Meas}}$. The series of measurement values $\{u_1(t_i)\}$ and $\{u_2(t_i)\}$ sampled within $t_0 < t < t_0 + T_{\mathrm{Meas}}$ have a sampling interval $\Delta t = t_i - t_{i-1} = 1/f_{\mathrm{s}} =$ const. with f_{s} denoting the sampling frequency. From both quadrature signals, the phase values $\varphi_{\mathrm{Mod}}(t)$ are calculated successively in the course of the measurement period using the following relationship:

$$\varphi_{\mathrm{Mod}}(t_i) = \arctan \frac{u_2(t_i)}{u_1(t_i)} + n\pi \tag{B.10}$$

where $n = 0, 1, 2, \ldots$

The procedures for the calculation of the arctan function with successive “phase-unwrapping” in particular (see reference [10]), are standard procedures in digital signal processing.

Using $\varphi_{\mathrm{Mod}}(t_i)$ obtained from equation (B.9), a series of discrete displacement values $\{s_{\mathrm{D}}(t_i)\}$ can be calculated by

$$s_{\mathrm{D}}\,(t_i) = \frac{\lambda}{4\pi}\,\varphi_{\mathrm{Mod}}(t_i) \tag{B.11}$$

If $\varphi_0 \neq 0$, then $\{s_{\mathrm{D}}(t_i)\}$ contains an offset. Because of the differentiation according to equation (B.8), this constant term does not affect the results for the velocity and the acceleration. The subscript D indicates that the values are disturbed by high-frequency noise. These disturbances are suppressed by discrete-time low-pass filtering.

The operations described in B.2 and B.3 are required to obtain the magnitude and phase shift of the complex sensitivity (frequency-domain version) and the shock sensitivity (time-domain version).

B.2 Discrete-time low-pass filtering method

To realize a low-pass filter procedure, an algorithm can be used for recursive computation of the output at any time t_i in terms of the previous outputs $y(t_{i-1})$, $y(t_{i-2})$, the current input sample $x(t_i)$ and previous input samples $x(t_{i-1})$, $x(t_{i-2})$:

$$y(t_i) = A_1 y(t_{i-1}) + A_2 y(t_{i-2}) + B_0 x(t_i) + B_1 x(t_{i-1}) + B_2 x(t_{i-2}) \quad \text{(B.12)}$$

where $i = 0, 1, \ldots, N-1$,

and A_1, A_2, B_0, B_1 and B_2 are the filter coefficients.

The frequency-response function of this second-order difference equation is defined by

$$H(\mathrm{j}\Omega) = \frac{B_0 + B_1 \mathrm{e}^{-\mathrm{j}\Omega} + B_2 \mathrm{e}^{-\mathrm{j}2\Omega}}{1 - A_1 \mathrm{e}^{-\mathrm{j}\Omega} - A_2 \mathrm{e}^{-\mathrm{j}2\Omega}} \quad \text{(B.13)}$$

where Ω denotes the normalized radian frequency $\Omega = 2\pi f / f_\mathrm{s}$.

To obtain a monotonous frequency response in the passband and stopband of this filter, a Butterworth function approximation can be used, given by

$$\left| H(\mathrm{e}^{\mathrm{j}\Omega}) \right|^2 = \frac{1}{1 + \left[\tan\left(\frac{\Omega}{2}\right) / \tan\left(\frac{\Omega_\mathrm{c}}{2}\right) \right]^4} \quad \text{(B.14)}$$

where Ω_c stands for the normalized cut-off frequency. Then the filter coefficients A_1, A_2 and B_0, B_1, B_2 are determined according to this approximating function. When corresponding design formulae are applied, their values are obtained depending on the desired cut-off frequency Ω_c.

The recursive computation of the output signal leads to a nonlinear phase shift. To satisfy the specification of a low-pass filter without any phase shift, the computation of the output signal is repeated in the reverse direction using the formula

$$y^*(t_{N-1-i}) = A_1 y^*(t_{N-2-i}) + A_2 y^*(t_{N-3-i}) + B_0 y(t_{N-1-i}) + B_1 y(t_{N-2-i}) + B_2 y(t_{N-3-i}) \quad \text{(B.15)}$$

where $i = 0, 1, \ldots, N-1$.

Then the resulting frequency-response function can be expressed as

$$H(\mathrm{e}^{\mathrm{j}\Omega}) \cdot H^*(\mathrm{e}^{\mathrm{j}\Omega}) = \left| H(\mathrm{e}^{\mathrm{j}\Omega}) \right|^2 \quad \text{(B.16)}$$

Thus, after applying the filter algorithm twice between the two signals $y^*(t_i)$ and $x(t_i)$, no phase shift occurs.

B.3 Differentiation method

Different procedures are available to carry out the derivation. The simplest of these, recommended in this part of ISO 16063, may be used if high-frequency disturbing influences are sufficiently suppressed. For this purpose, the discrete-time low-pass filtering described in B.2 has been introduced. After discrete low-pass filtering of the displacement values obtained from equation (B.10), leading to a series of "smooth" displacement values denoted by $\{s(t_i)\}$, the differentiation may be carried out once according to the formula

$$v_{\mathrm{D}}(t_i) = \frac{1}{2\Delta t}\left[s(t_{i+1}) - s(t_{i-1})\right] \qquad \text{(B.17)}$$

The subscript D indicates that the values obtained by differentiation are disturbed by high-frequency noise. The filtering operation must, therefore, be applied to these velocity values $\{v_{\mathrm{D}}(t_i)\}$ to obtain "smooth" values $\{v(t_i)\}$. Under these conditions, the simple expression for the differentiation may be used again to obtain the acceleration:

$$a(t_i) = \frac{1}{2\Delta t}\left[v(t_{i+1}) - v(t_{i-1})\right] \qquad \text{(B.18)}$$

B.4 Alternative differentiation method

Another method to obtain the first derivative $x'(t_i)$ of a time series $x(t_i)$ for $i = 0, \ldots, L-1$ (for example, a Gaussian-like velocity series $\{v(t_i)\}$ consists of following signal processing steps.

a) Calculate the complex spectrum $X(\mathrm{j}2\pi f)$ of the time series for $f_n = \frac{f_{\mathrm{s}}}{L} n$ by applying the discrete Fourier transform (DFT):

$$X(\mathrm{j}2\pi f_n) = \sum_{i=0}^{L-1} x(t_i) \mathrm{e}^{-\mathrm{j}2\pi \frac{f_n}{f_{\mathrm{s}}} i} \qquad \text{(B.19)}$$

where $0 \leqslant n \leqslant L-1$.

b) Multiply the complex spectrum $X(\mathrm{j}2\pi f_n)$ by the complex radian frequency $\mathrm{j}2\pi f_n$ to obtain the complex spectrum of the first derivative:

$$X'(\mathrm{j}2\pi f_n) = \mathrm{j}2\pi f_n \times X(\mathrm{j}2\pi f_n) \qquad \text{(B.20)}$$

where $0 \leqslant n \leqslant L-1$.

c) Apply the inverse discrete Fourier transform (IDFT) to $X'(\mathrm{j}2\pi f)$ to obtain the derivative of the time sequence:

$$x'(t_i) = \frac{1}{L} \sum_{n=0}^{L-1} X'(\mathrm{j}2\pi f_n) \mathrm{e}^{-\mathrm{j}2\pi \frac{f_n}{f_{\mathrm{s}}} i} \qquad \text{(B.21)}$$

where $0 \leqslant i \leqslant L-1$.

The latter method suppresses the influence of disturbing signals on the differentiation of the time sequence to be suppressed. It may be applied to calculate the derivative of Gaussian-like velocity impulses of low level shocks.

Annex C
(informative)

Alternative method of calculation of magnitude and phase shift of the complex sensitivity

C.1 The magnitude and, if the conditions of C.2 are fulfilled, also the phase shift of the complex sensitivity of the accelerometer can be obtained using the intermediate results of step e) in 7.3.3. The amplitudes and initial phases obtained from the complex frequency spectrum of the acceleration at the frequencies f_n are denoted by

$$\widehat{a}_n, \ \varphi_{a,n}$$

where

$$\widehat{a}_n = \widehat{a}(f_n), \ \varphi_{a,n} = \varphi_a(f_n) \tag{C.1}$$

The calculation steps required are as follows.

a) Calculate the complex frequency spectrum of the accelerometer output by DFT applied to the series $\{u(t_i)\}$ of the filtered accelerometer output values. The resulting amplitudes and phases of the acceleration at the frequencies f_n are denoted by

$$\widehat{u}_n, \ \varphi_{u,n}$$

where

$$\widehat{u}_n = \widehat{u}(f_n), \ \varphi_{u,n} = \varphi_u(f_n) \tag{C.2}$$

b) Calculate the series of values of magnitude $\widehat{S}_n = \widehat{S}(f_n)$ and phase shift $\Delta\varphi_n = \Delta\varphi(f_n)$ (where $n = 0, 1, 2, \ldots, N-1$) of the complex sensitivity of the accelerometer using the formulae

$$\widehat{S}_n = \widehat{u}_n / \widehat{a}_n \tag{C.3}$$

$$\Delta\varphi_n = \varphi_{u,n} - \varphi_{a,n} \tag{C.4}$$

When the calibration results are reported, the expanded uncertainty of measurement shall be calculated and reported in accordance with ISO 16063-1.

C.2 The three sampling processes shall start and end at the same points of time and, at least for both interferometer signals, shall be synchronized by a single-system clock.

To eliminate the disturbing influence of the phase response of the filter, the filtering operation shall be carried out in both the forward and reverse counting directions of the values within the series (cf. annex B). This applies to the filtering of both the series of measuring signals from the interferometer and that from the accelerometer output. To realize a Butterworth filter of the fourth order, both filtering operations should be of the second order.

C.3 The above relationships are based on the description of the discrete Fourier transform given in annex B with the following specifications. The series of discrete Fourier coefficients of the sampled accelerometer output signal $X_u(f_n)$ and the series of Fourier coefficients of the sampled velocity signal $X_v(f_n)$ determine the complex sensitivity of the accelerometer to be calibrated, by the formula

$$\underline{S}(f_n) = \frac{X_u(f_n)}{\mathrm{j}2\pi f_n X_v(f_n)} \tag{C.5}$$

where $0 < n \leqslant L-1$.

To obtain the magnitude and phase shift of the complex sensitivity, equation (C.5) is re-written as follows:

$$\underline{S}(f_n) = \frac{|X_u(f_n)|\, \mathrm{e}^{\mathrm{j}\varphi_u(f_n)}}{|2\pi f_n X_v(f_n)|\, \mathrm{e}^{\mathrm{j}\left[\varphi_v(f_n)+\frac{\pi}{2}\right]}} \tag{C.6}$$

By using the symbols introduced at the beginning of annex B, the magnitude of the complex sensitivity can be expressed by

$$\widehat{S}_n = \frac{\widehat{u}_n}{\widehat{a}_n} = \frac{|X_u(f_n)|}{|2\pi f_n X_v(f_n)|} \tag{C.7}$$

and the phase shift by

$$\Delta\varphi_n = \varphi_{u,n} - \varphi_{a,n} = \varphi_u(f_n) - \varphi_v(f_n) - \frac{\pi}{2} \tag{C.8}$$

NOTE The above relationships and equations (B.5) and (B.9) in annex B in particular, presuppose ideal conditions which are not fulfilled in reality. Under practical conditions, the signals from the photodetectors deviate with respect to their amplitudes $\widehat{u}_1$, $\widehat{u}_2$ and the nominal phase shift $\pi/2$, and different offsets $u_{0,1}$, $u_{0,2}$ can occur. The influences from non-ideal quadrature signals within the tolerance ranges stated in 4.6 are described in reference [6].

Bibliography

[1] VON MARTENS H.-J., SCHLAAK H.-J. and TÄUBNER A. Interferometrische Kalibrierung von Translations- und Rotationsaufnehmern mit Sinus- und Stoßanregung. *Fortschritte der Akustik, DAGA 94*, part B, 1994, pp. 681-684

[2] HARRIS C. M. and CREDE Ch. E. *Shock and Vibration Handbook*, 3rd edn., McGraw-Hill, New York, Toronto, London, 1987

[3] EVANS D. J. Testing the sensitivity of accelerometers using mechanical shock pulses under NIST special publication 250 special test No. 24040S. *ASME International Mechanical Engineering Congress & Exposition*, San Francisco, California, 1995

[4] KOLSKY H. *Stress waves in solids*. Dover Publications, New York, 1963, p. 215

[5] SILL R. D. Shock calibration of accelerometers at amplitudes to 100 000 g using compression waves. *Proceedings of the 29th International Instrumentation Symposium*, Albuquerque, New Mexico, 1983; *Instrument Society of America, Instrumentation in the Aerospace Industry*, **29**, pp. 503-516

[6] LINK A., VON MARTENS H.-J. and WABINSKI W. New method for absolute shock calibration of accelerometers. *SPIE*, **3411**, 1998, pp. 224-235

[7] WABINSKI W. and VON MARTENS H.-J. Time interval analysis of interferometer signals for measuring amplitude and phase of vibrations. *SPIE*, **2868**, 1996, 166-177

[8] LINK A., GERHARDT J. and VON MARTENS H.-J. Amplitude and phase calibration of accelerometers in the nanometer range. *SPIE*, **2868**, 1996, pp. 37-48

[9] GLÖCKNER B., VON MARTENS H.-J., ROGAZEWSKI P., SCHLAAK H.-J., WABINSKI W. and TÄUBNER A. Neue Verfahren zur Kalibrierung von Stoßmeßmitteln. In: *Metrologische Abhandlungen*, **8**, No. 3, 1988, pp. 245-258

[10] TRIBOLET J. M. A new phase unwrapping algorithm. *IEEE Transactions on Acoustics, Speech, and Signal Processing*, ASSP-25, No. 2, April 1977, pp. 170-177

[11] Guide to the expression of uncertainty in measurement. BIPM, IEC, IFCC, ISO, IMPAC, IMPAP, OIML, 1993

[12] VON MARTENS H.-J. and ROGAZEWSKI P. Representation and transfer of the units of vibration quantities in the GDR. *Bulletin OIML*, No. 108, Sept. 1987, pp. 26-37

[13] WEIßENBORN Ch. Verbesserte Impulsformung bei der Kalibrierung von Beschleunigungsaufnehmern. *Technisches Messen*, **66**, 1999, pp. 277-285

[14] ISO 5347-4:1993, *Methods for the calibration of vibration and shock pick-ups — Part 4: Secondary shock calibration*[1)]

1) To be revised as ISO 16063-22.

ICS 17.160

Price based on 22 pages